Pressure-dependent phonon properties of III-V compound semiconductors

Devki N. Talwar
Department of Physics, Indiana University of Pennsylvania, Indiana, Pennsylvania 15705-1087

Michel Vandevyver
Département de Physico-Chimie, Centre d'Etudes Nucléaire de Saclay, Boîte Postale 2, 91191 Gif-sur-Yvette CEDEX, France

(Received 21 September 1989; revised manuscript received 8 February 1990)

Using a phenomenological lattice-dynamical theory in the *quasiharmonic approximation*, we present a comprehensive study to understand the effects of pressure on the vibrational properties of Ga-In pnictides that exhibit a sphalerite crystal structure. The existing pressure-induced Raman scattering data for phonon frequencies, the ultrasonic measurements of elastic and lattice constants, are used as constraints to stringently test the reliability of our *rigid-ion model*. The effects of high pressure on phonon dispersion curves are shown to lead to a softening in the transverse acoustic modes. At low temperatures this provides a possible driving mechanism for the decrease in the Debye temperature and the occurrence of a *negative* Grüneisen constant and thermal-expansion coefficient in semiconductors. With a few exceptions (InP, GaAs, and GaSb), our calculated values for several elemental and compound semiconductors have qualitatively satisfied the empirical linear relationship between the Grüneisen parameter $\gamma_{TA(X)}$ and the transition pressure P_t. Numerical results for the lattice dynamics, one-phonon and two-phonon density of states, Debye temperature, Grüneisen constant, and linear thermal-expansion coefficient are all shown to be in reasonably good agreement with the existing experimental data.

I. INTRODUCTION

The use of a diamond anvil cell, the ruby fluorescence pressure scale, optical-absorption and -reflectivity measurements, inelastic light scattering (Raman and Brillouin), and x-ray diffraction techniques have stimulated considerable interest in the high-pressure studies[1-3] for the electrical and vibrational properties of semiconductors. Since the available pressure ranges are so high ($\sim$300 kbar), one may, in principle, observe many new phenomena concerning the behavior of solids which otherwise could not be measured. For example, the shifts in the energy gap with pressure have been reported in recent years using optical-absorption and -luminescence measurements.[4,5] These studies, along with the pressure dependence of impurity levels, have provided us with a unique method to identify the site selectively and the symmetry of defects in semiconductors.

For extracting information regarding the vibrational properties[6-9] at high pressure, Raman scattering is probably the most amenable method, from among the various available techniques. Cardona and his co-workers[10-15] have recently used Raman spectroscopy to observe the effects of pressure on the lattice dynamics of III-V compounds up to their phase transition pressure P_t. Whenever phase transitions occur, Raman scattering reveals them as discontinuities in the frequency and/or the intensity of the phonon peaks. From the critical-point analyses of the pressure dependent one- and two-phonon Raman scattering spectra, the authors of Refs. 10–15 have obtained information about the longitudinal- and transverse-optical-mode Grüneisen (γ_{LO} or γ_{TO}) parameters. Some ultrasonic measurements have also been reported for the pressure-dependent lattice and elastic stiffness constants.[16-21] For example, Novikova[22] and others[23] have provided us with extensive experiments for the linear thermal-expansion coefficient [$\alpha(T)$] in several II-VI, III-V, and IV-IV crystals. One of the conspicuous properties observed for these materials is the negative $\alpha(T)$ for temperatures below $T<0.07\Theta_0$, where Θ_0 is the limiting value of the Debye characteristic temperature as $T\rightarrow 0$ K. Despite a wealth of information about the pressure-dependent vibrational properties,[1-23] very few *realistic* theoretical attempts[24-28] have been made to understand the existing experimental data. To extract knowledge on the interatomic binding forces in compound semiconductors under compression and to relate that information to charge transfer effects and structural instabilities, the above experimental results provide us a good testing ground for theoretical[24-28] studies which, in the past, have been rather sparse.

Two numerical techniques have been developed in recent years for treating the pressure-dependent phonon properties in semiconductors. The first technique deals with the phenomenological lattice-dynamical models[24,25] and the second one derives the phonon energies *ab initio*.[26-28] In the latter approach,[26-28] the total energy is computed for the equilibrium atomic configuration and for the configuration distorted by a given eigenvector. The harmonic expansion of the energy difference provides the phonon frequency at that volume. For phonons in GaAs, the only available *self-consistent* calculation in the Hohenberg-Kohn-Sham local-density-functional (LDF) formalism is that of Kunc and Martin.[28] It may

be noted that the results for various physical properties in their study are well understood with the exception of the calculated value of $\gamma_{TA(X)} = -3.48$ which is negative, but too large. The authors of Ref. 28 have concluded that for transverse acoustic phonons in GaAs, the anharmonic contributions are very important. In imperfect semiconductors, except for a few recent studies of estimating lattice relaxation,[29-31] there still remain several vibrational properties to be understood by the *microscopic* methods. On the other hand, all the reasonably successful calculations in the Green's-function framework[32-34] for the impurity modes, impurity-induced infrared absorption, and/or Raman scattering spectra, etc., use the *macroscopic* theories.

In an earlier study,[35] we treated the pressure-dependent vibrational properties of zinc chalcogenides (ZnS, ZnSe, and ZnTe) by using a phenomenological lattice dynamical theory. In this paper, we have reasserted the reliability of our eleven-parameter rigid-ion model (RIM11)[35,36] and reported for the first time the effect of pressure on the dynamical behavior of III-V (GaP, GaAs, GaSb, InP, InAs, and InSb) compound semiconductors. At pressure $P=0$, an accurate set of model parameters for Ga-In pnictides fitted mostly to the inelastic neutron scattering measurements,[37-42] have been obtained. The parameter values of the RIM11 at $P \neq 0$ are derived by incorporating the pressure-dependent critical-point phonon energies from the first- and second-order Raman data,[10-15] and the elastic and lattice constant values[16-20] from the ultrasonic measurements. In the *quasiharmonic approximation,* the present theoretical treatment has been able to predict reasonably well the lattice dynamics and related properties of III-V compounds at any P, up to their phase transition pressure P_t. The calculated results for various quantities, viz., one- and two-phonon density of states, Debye temperature, Grüneisen parameter, and thermal-expansion coefficient are compared and discussed with the existing experimental data.[10-23] Except in the high-temperature region where the anharmonic effects dominate, the theoretical values of $\alpha(T)$ in most of the systems studied here agree reasonably well with the low-temperature data.[22,23]

II. BASIC THEORY OF THERMAL EXPANSION IN SOLIDS

A. Mode Grüneisen parameters

In describing the volume or pressure dependence of the phonon frequencies in solids, Barron[43] has introduced the

TABLE I. Calculated RIM parameters (10^5 dyn cm^{-1}) ($A, B, C_1, \ldots, Z_{eff}$) for the lattice dynamics of Ga and In pnictides (GaP, GaAs, GaSb, InP, InAs, and InSb) in the notations of Kunc (Ref. 36). The lattice parameter a is in Å.

Model	GaP		GaAs		GaSb	
parameter	1 atm[a]	220 kbar[b]	1 atm[a]	185 kbar[b]	1 atm[a]	67 kbar[b]
a_0	2.725	2.5807	2.8265	2.6775	3.0480	3.027 55
A	−0.4519	−0.733 85	−0.4071	−0.730 84	−0.3560	−0.4604
B	−0.4527	−0.780 00	−0.1660	−0.350 00	−0.2620	−0.3500
C_1	−0.0425	−0.069 80	−0.0177	−0.054 95	−0.0190	−0.0338
C_2	−0.0352	−0.066 30	−0.0461	−0.037 10	−0.0280	−0.0365
D_1	−0.0912	−0.144 00	0.0248	0.029 10	−0.0668	−0.0982
D_2	0.0303	0.001 00	−0.1233	−0.166 00	0.0230	0.0230
E_1	0.1055	0.153 50	0.0912	0.146 00	0.0700	0.1030
E_2	−0.1788	−0.190 00	0.0834	0.118 00	−0.1200	−0.1620
F_1	0.1404	0.235 00	−0.1172	−0.166 00	0.1300	0.1800
F_2	−0.2027	−0.331 00	0.2008	0.347 00	−0.1190	−0.1520
Z_{eff}	0.7100	0.6134	0.6580	0.576 70	0.4840	0.4322
Model	InP		InAs		InSb	
parameter	1 atm[a]	85 kbar[b]	1 atm[a]	40 kbar[b]	1 atm[a]	22.5 kbar[b]
a_0	2.931 85	2.8325	3.018 00	2.965 90	3.241 00	3.192 70
A	−0.365 00	−0.474 66	−0.345 00	−0.414 00	−0.291 30	−0.325 80
B	−0.100 00	−0.110 00	−0.250 00	−0.259 50	−0.178 60	−0.200 00
C_1	−0.017 00	−0.025 40	−0.019 50	−0.019 74	−0.027 20	−0.031 00
C_2	−0.043 00	−0.057 10	−0.007 50	−0.010 36	−0.008 00	−0.008 50
D_1	−0.003 00	−0.000 81	0.011 30	−0.002 60	−0.005 90	−0.011 30
D_2	−0.120 00	−0.182 00	−0.059 00	−0.071 57	−0.041 00	−0.004 70
E_1	0.050 00	0.085 00	−0.053 00	−0.050 90	0.071 10	0.065 00
E_2	0.110 00	0.156 00	0.055 00	0.074 52	0.030 50	0.041 00
F_1	−0.071 00	−0.091 00	−0.077 00	−0.097 00	−0.074 40	0.0810
F_2	0.177 00	0.255 00	0.099 30	0.149 60	0.116 60	0.132 00
Z_{eff}	0.820 00	0.785 00	0.756 00	0.722 00	0.583 80	0.554 30

[a]References 49–54.
[b]Present study.

TABLE II. Physical constants needed for the evaluation of the RIM11 parameters and various other lattice dynamical properties of Ga and In pnictides. The experimental values (Ref. 36) of the elastic constants C_{11}, C_{12}, C_{44}, bulk modulus B_T (in the units of 10^{11} dyn cm^{-2}), and their pressure derivatives C'_{11}, C'_{12}, C'_{44}, and B'_T (Refs. 16–21) are given.

Quantity	GaP	GaAs	GaSb	InP	InAs	InSb
C_{11}	14.12	11.81	8.849	10.22	8.329	6.717
C_{12}	6.253	5.32	4.387	5.76	4.526	3.665
C_{44}	7.047	5.94	4.325	4.60	3.959	3.018
C'_{11}	4.77	4.63	5.000	4.17	4.30[a]	4.43
C'_{12}	4.79	4.62	4.700	4.80	4.725[a]	4.65
C'_{44}	0.92	1.10	1.000	0.36	0.414[a]	0.467
B_T	8.87	7.48	5.635	7.247	5.96[a]	4.68
B'_T	4.79	4.67	4.750	4.59	4.59[a]	4.58

[a]Average values considered between InP and InSb.

mode Grüneisen parameter γ_i.[44] Following Born's dynamical theory of crystal lattices,[45] the author of Ref. 43 defined γ_i for the ith mode with phonon frequency ω_i, in the following way:

$$\gamma_i = -\frac{d\ln\omega_i}{d\ln\Omega} = \frac{B_T\, d\omega_i}{\omega_i\, dP} = -\frac{d\ln\Omega^{-1/3} v_i}{d\ln\Omega} , \tag{1}$$

where B_T is the isothermal bulk modulus, Ω is the volume of the crystal, P is the pressure, and v_i is the propagation velocity of the ith wave ($i=1,2,3$). At low temperatures $T\to 0$, where only the acoustic waves are important, the limiting value of the Grüneisen constant γ_0 will take the form

$$\gamma_0 = \frac{\int\int \sum_{i=1}^{3} \gamma_i v_i^{-3}\, d\omega}{\int\int \sum_{i=1}^{3} v_i^{-3}\, d\omega} . \tag{2a}$$

Similarly at high temperatures $T\to\infty$, the value of the Grüneisen constant γ_∞ may be expressed as

$$\gamma_\infty = \frac{1}{3N}\sum_{i=1}^{3}\gamma_i , \tag{2b}$$

where N is number of atoms in a solid. The dimensionless quantity γ_i defined in Eq. (1) can be obtained, in gen-

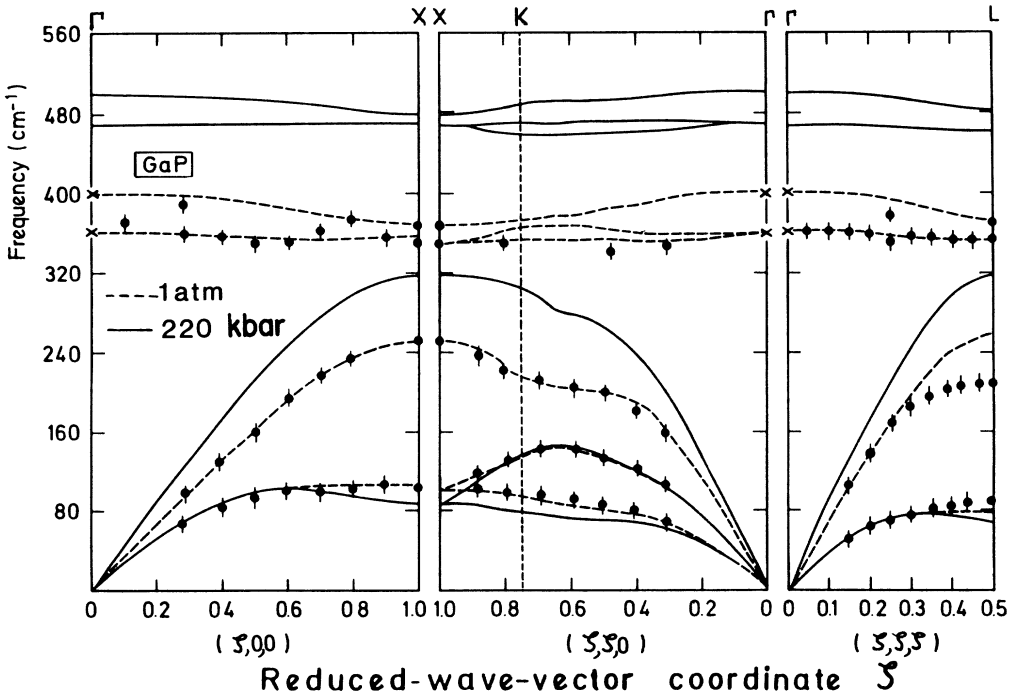

FIG. 1. RIM11 calculations for the phonon dispersions along high symmetry directions for GaP. The dotted curves represent the inelastic neutron scattering (Ref. 38) (1 atm) fit whereas the solid curves show the calculations for 220 kbar with parameter values given in Table I.

eral, from the measured pressure dependence of the mode frequency ω_i and B_T. On the other hand, in the Debye's formulation, the average Grüneisen constant $\bar{\gamma}$ is related to γ_i as

$$\bar{\gamma}=\frac{\sum_{i=1}^{3}\gamma_i C_i}{\sum_{i=1}^{3}C_i}=\frac{\beta\Omega B_T}{C_\Omega}\ , \tag{3}$$

where C_i is the heat capacity of a single harmonic oscillator of frequency ω_i,

$$C_i=Nk_B\left[\frac{\hbar\omega_i}{k_BT}\right]^2\frac{\exp\left[-\frac{\hbar\omega_i}{k_BT}\right]}{\left[1-\exp\left[\frac{\hbar\omega_i}{k_BT}\right]\right]^2}\ , \tag{4}$$

and C_Ω is the crystal heat capacity at constant volume with β $(=3\alpha)$ as the volume thermal-expansion coefficient. If the mode Grüneisen parameters are known in a solid for all of its branches throughout the Brillouin zone (cf. Sec. II C), the thermal expansion can be easily obtained from Eq. (3).

B. Effective charge and its pressure dependence

Under compression, the change in splitting of the optical phonon frequencies at the center of the Brillouin zone $[\omega_{\mathrm{LO}(\Gamma)}-\omega_{\mathrm{TO}(\Gamma)}]$ may cause a redistribution of the Szigetti's effective charge (e_s^*) on the ions that, in turn, can affect the ionicity (covalency) of heteropolar semiconductors. An equivalent quantity, known as the Born's transverse dynamic charge e_T^* $[=e_s^*(\epsilon_\infty+2)/3]$, is also a measure of the ionicity (covalency) in polar crystals. This is defined as[6]

$$\omega^2_{\mathrm{LO}(\Gamma)}-\omega^2_{\mathrm{TO}(\Gamma)}=\frac{4\pi e_T^{*2}N}{\epsilon_\infty\mu\Omega}\ , \tag{5}$$

where the term ϵ_∞ is the high-frequency or optical (electronic) dielectric constant for the frequencies well above the $\omega_{\mathrm{LO}(\Gamma)}$ but below the optical absorption edge, i.e., the dielectric constant in the absence of lattice vibrations; and μ is the reduced mass of the crystal. With an explicit use of the Lydane-Sachs-Teller relation $\omega^2_{\mathrm{LO}}/\omega^2_{\mathrm{TO}}=\epsilon_0/\epsilon_\infty$, where ϵ_0 is the static dielectric constant in the limit of zero frequency, Eq. (5) can take the form

$$\epsilon_0=\epsilon_\infty+\frac{4\pi e_T^{*2}N}{\mu\Omega\omega^2_{\mathrm{TO}(\Gamma)}}=\epsilon_\infty+\epsilon_{\mathrm{lat}}\ . \tag{6}$$

Here, ϵ_{lat} is the lattice contribution to the dielectric constant. In heteropolar semiconductors, the term ϵ_{lat} arises from the fact that the LO(Γ) mode produces a macroscopic electric moment which separates it in energy from the TO(Γ) mode. For homopolar crystals, viz., Si, where there is a center of inversion symmetry between the atoms, $\omega_{\mathrm{LO}(\Gamma)}=\omega_{\mathrm{TO}(\Gamma)}$, the lattice vibrations make no contribution to ϵ_0. Consequently, $\epsilon_0=\epsilon_\infty=n^2$, where n is known as the index of refraction.

From Eq. (6), it is quite evident that ϵ_{lat} and its pres-

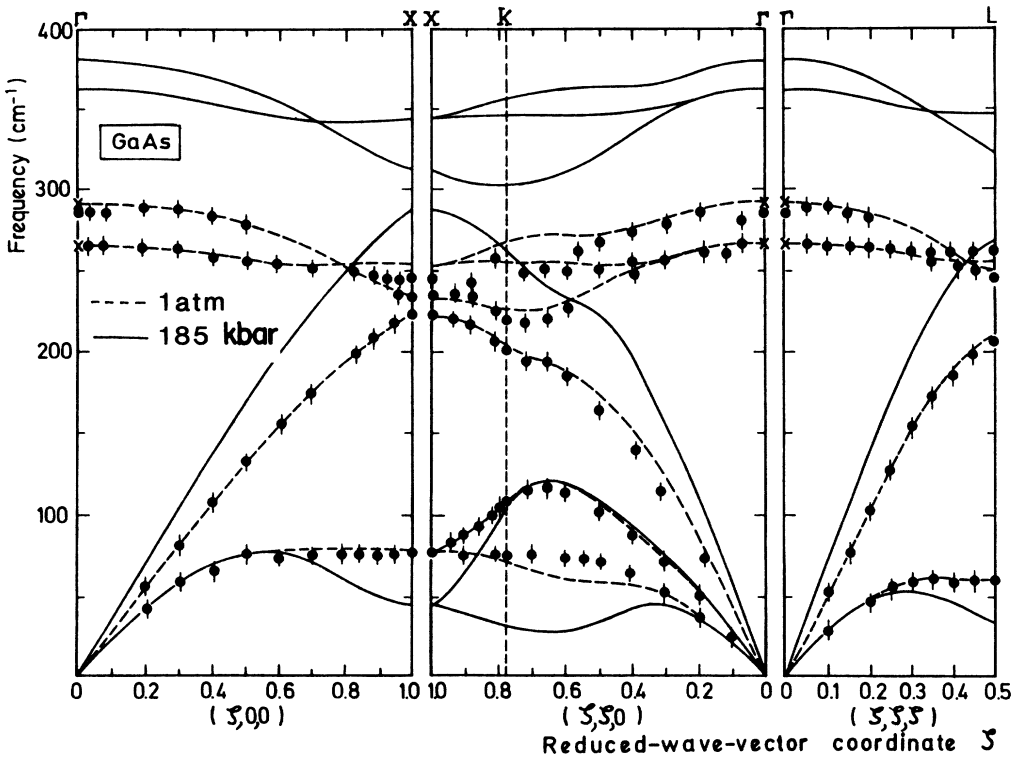

FIG. 2. Same key as of Fig. 1 for GaAs (1 atm and 185 kbar).

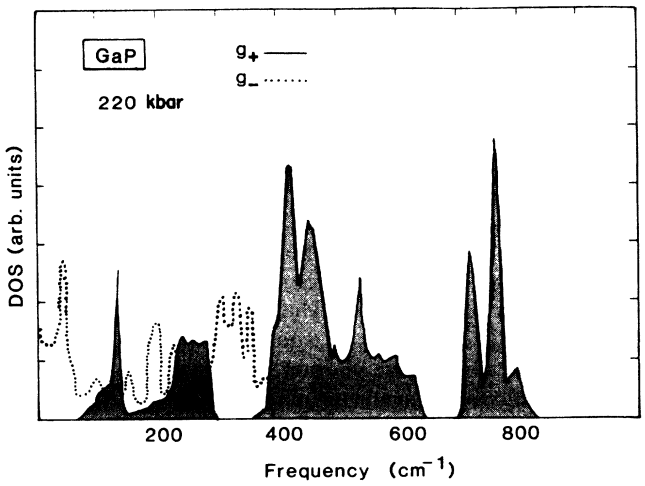

FIG. 3. Calculated two-phonon subtractive (· · ·) and additive (——) density of states for GaP. The major peaks show the shift of participating critical-point phonons under compression. The shift in optical phonons are consistent with the existing Raman data (see text).

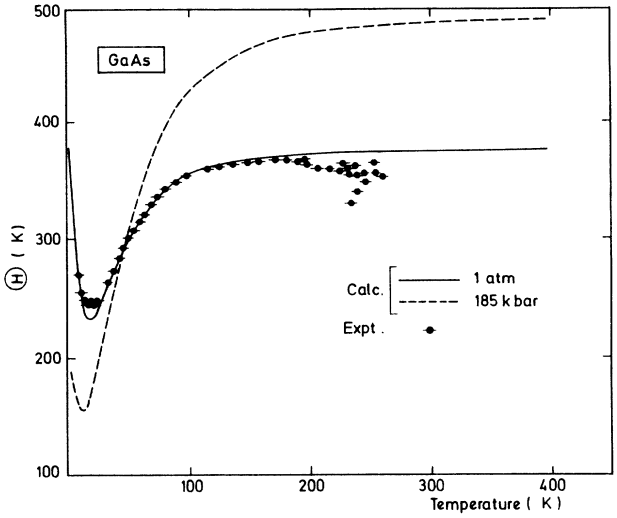

FIG. 5. Calculated variation of Debye temperature [$\Theta(T)$] vs temperature for GaAs (1 atm and 185 kbar) using the parameter values of Table I. Experimental data are taken from Ref. 56.

sure dependence can be derived by using the relation

$$\frac{\partial \ln \epsilon_0}{\partial P} = \frac{\epsilon_\infty}{\epsilon_0}\frac{\partial \ln \epsilon_\infty}{\partial P} + \frac{\epsilon_{\rm lat}}{\epsilon_0}\frac{\partial \ln \epsilon_{\rm lat}}{\partial P} , \tag{7}$$

if ϵ_0, ϵ_∞, and their respective pressure variations are known. Once the pressure dependence of $\epsilon_{\rm lat}$ is obtained, one can easily predict the effect of compression on the covalency (ionicity or e_T^*) of the semiconductor bond by [cf. Eq. (6)],

$$\frac{\partial \ln e_T^*}{\partial T} = \frac{1}{2}\frac{\partial \ln \epsilon_{\rm lat}}{\partial P} + \frac{\partial \ln \omega_{\rm TO(\Gamma)}}{\partial P} - \tfrac{1}{2}\chi_T , \tag{8a}$$

or

$$\gamma_{e_T^*} = \tfrac{1}{2}\gamma_{\rm lat} + \gamma_{\rm TO(\Gamma)} - \tfrac{1}{2} , \tag{8b}$$

where χ_T ($=1/B_T$) is the volume compressibility and the term $\gamma_{e_T^*}$ is the Grüneisen parameter for the Born's dynamic charge. The effect of pressure on the bonding mechanism in semiconductors may also be learned from a reliable lattice-dynamical study (cf. Sec. III B).

C. Vibrational models in the quasiharmonic approximation

In a lattice-dynamical model, the potential energy is a function of atomic positions only and contains terms up to second order (harmonic approximation) in atomic displacements. In the *harmonic approximation*, the normal modes are the superposition of independent vibrations, whose symmetry clearly indicates that there can be no thermal expansion. The second-order coefficients, and hence the frequencies of the modes, are unaltered by any constant external forces. They are, therefore, independent of the volume. Vibrational thermal expansion occurs only in the *anharmonic models*. In the presence of

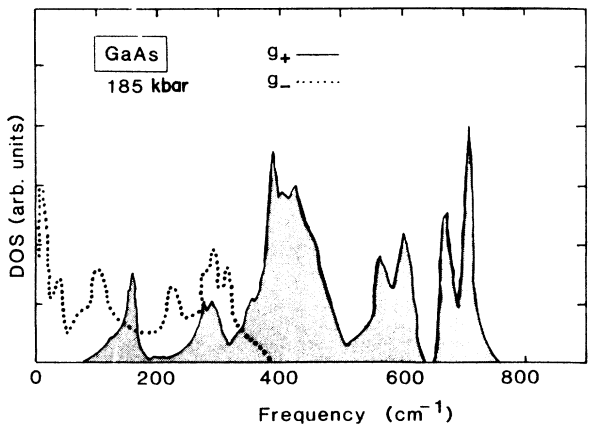

FIG. 4. Same key as of Fig. 3 for GaAs.

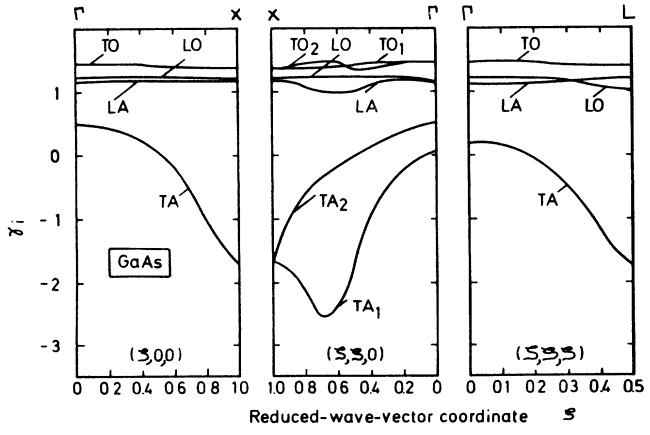

FIG. 6. Calculated Grüneisen parameter along high-symmetry directions for GaAs.

anharmonicity, the second-order coefficients are volume dependent. To a first approximation, the thermal expansion for weakly *anharmonic* vibrations can be obtained in terms of the *quasiharmonic* theory of Leibfreid and Ludwig.[46] In this theory we treat the vibrations as harmonic but we assume volume- or pressure-dependent frequencies $\omega_i(\Omega$ or $P)$.

In a crystalline solid, since each mode is labeled by $\omega_i(\mathbf{q})$ therefore, an individual Grüneisen parameter $\gamma_i(\mathbf{q})$ or the average Grüneisen constant $\bar{\gamma}(T)$ may be calculated approximately using the Eqs. (1)–(3). Here, $\mathbf{q}$ is the wave vector and i denotes the phonon branch index. To calculate $\bar{\gamma}(T)$ and/or $\alpha(T)$, the integration is to be performed over the first Brillouin zone and this can be done following the standard numerical methods.[47,48]

Rigid-ion model

The field of phenomenological models for lattice dynamics has been well established for years. It is worth pointing out, however, that the model one should select for the bulk phonon must be capable of giving realistic phonon modes within a physically sensible framework. There are a number of such methods available, of course, but all are characterized by a requirement that nearest-neighbor forces are not sufficient in semiconductors. Second nearest-neighbor forces (to include bond bending) are a minimal requirement in any physically reasonable scheme. The most economical and, probably, a more physically meaningful among the different mechanical methods of interatomic interactions used in compound semiconductors, is the rigid-ion model. In addition to purely short-range forces (with interactions up to and including second neighbors), the RIM force constant matrix contains a contribution from the classical electrostatic (Coulomb) interactions. The particular version of the RIM (Ref. 36) that we have considered here for studying the pressure-dependent phonon properties in III-V compound semiconductors is similar to the one used earlier for zinc chalcogenides.[35]

The set of eleven RIM-model parameters ($A,B,C_1,\ldots,Z_{\text{eff}}$) for III-V compounds at ambient pressure were determined[49–54] with the aid of elastic stiffness constants (C_{ij}), zone-center and zone-boundary phonon frequencies (ω's), and lattice parameter (a_0). For studying the parametric dependences on P, we have used the critical-point phonon energy values (derived either from the high pressure Raman measurements[10–15] and/or from reliable theoretical schemes) as input and considered the experimentally known pressure-dependent

TABLE III. Glossary of the calculated Grüneisen parameters for III-V compound semiconductors using *macroscopic theory* (see text). The results are compared with the pressure-Raman scattering (Refs. 10–15) and existing theoretical data (Ref. 26). Branches (in order of descending energy) and critical points are arranged to match the usual phonon dispersion format.

Critical point	Mode	GaP Expt.[a]	GaP Our	GaAs Expt.[a]	GaAs Calc.[b]	GaAs Our	GaSb Expt[a]	GaSb Our
Γ	LO	0.95±0.02	0.96	1.23±0.02	1.78	1.24	1.21±0.02	1.06
	TO	1.09±0.03	1.19	1.39±0.02		1.46	1.23±0.02	0.21
X	LO		1.17			1.23		1.42
	TO	1.30	1.30	1.73		1.39		1.26
	LA	1.0	1.00		1.30	1.18		1.12
	TA	−0.72±0.03	−0.68	−1.62±0.05	0.53	−1.67		−0.98
L	LO		1.17			1.03		1.43
	TO	1.50	1.24	1.50		1.43		1.21
	LA		0.94		1.29	1.24		1.05
	TA	−0.81±0.07	−0.49	−1.72±0.15	0.23	−1.70		−1.17

Critical point	Mode	InP Expt.[a]	InP Calc.[b]	InP Our	InAs Expt.[a]	InAs Our	InSb Expt.[a]	InSb Calc.[b]	InSb Our
Γ	LO	1.24		1.04	1.06	1.14	1.17		1.05
	TO	1.44		1.34	1.21	1.43	1.41		1.26
X	LO			1.22		1.04			1.83
	TO	1.40		1.26		1.23			1.73
	LA		1.30	1.17		1.31			0.60
	TA	−2.10	0.11	−1.07		−2.24		−2.10	−2.37
L	LO			1.07		1.56			1.28
	TO	1.40		1.33		1.10			1.19
	LA		1.20	1.34		0.70			1.07
	TA	−2.0	−0.27	−2.41		−1.75		−2.00	−1.77

[a]References 10–15.
[b]Reference 26.

TABLE IV. Calculated values of α_{min} (10^6 deg^{-1}) and $d\Theta/dP$ (deg/kbar) for various III-V compounds. The theoretical results of $\gamma_{TA(X)}$ along with the available transition pressure P_t (kbar) for each compound are also given.

Compound	α_{min} Calc.[a]	α_{min} Expt.[b]	$d\Theta/dP$ 300 K	P_t	$\gamma_{TA(X)}$	$\gamma_{TA(L)}$
GaP	−0.08		0.62	220	−0.68	−0.49
GaAs	−0.49	−0.5	0.60	185	−1.67	−1.70
GaSb	−0.45	−1.0	0.64	67	−0.98	−1.17
InP	−1.13		0.66	85	−1.07	−2.41
InAs	−1.57	−1.0	0.62	40	−2.24	−1.75
InSb	−2.0	−1.6	0.59	22.5	−2.37	−1.77

[a]The present work.
[b]References 22 and 23.

elastic-$\{C_{ij}\}$ and lattice-$\{a\}$ constant values[16–23] as constraint (cf. Sec. III A).

III. NUMERICAL COMPUTATIONS AND RESULTS

A. Rigid-ion-model parameters

The unique set of neutron-fitted rigid-ion-model parameters in GaP, GaAs, GaSb, InP, InAs, and InSb have already been obtained[49–54] at ambient pressure (see Table I). This has helped us in establishing the new set of values for $P\neq 0$. In estimating the $P\neq 0$ parameters, we started with the extrapolation formula of Murnaghan[55] and expressed the lattice constant a under pressure P as

$$\frac{a}{a_0}=\left[\frac{B_T'}{B_T}P+1\right]^{-1/3B_T'}, \tag{9}$$

where B_T' is the pressure deviative of B_T. Using Eq. (9) along with the physical parameters given in Table II, the pressure variation of the volume ratio V/V_0 is calculated for several III-V compounds. For comparable cases (GaAs, GaSb, and InSb), the agreement with the existing experimental data of McSkimin and co-workers[18] and Peresada[19] is excellent. This leads us to believe that the pressure derivatives of the crystal volume for GaP and In pnictides will be equally reliable. It is worth mentioning that, except at Γ point, the experimental data for the pressure variation of phonon energies at X- and L-critical points are not known for all the III-V compounds. However, reasonably accurate values are available in the literature for Si, Ge, GaP, and several II-VI compounds.[10–15] These frequencies are generally obtained from investigations of the variation of second-order Raman spectrum with P. By relating the known pressure-dependent critical-point phonon frequencies with the elastic and lattice constants [see, for example, Ref. 41(b) and references therein], we were able to calculate approximately the required energy values of the zone boundaries for all the III-V compounds. In evaluating the new set of RIM11 parameters for $P\neq 0$, the pressure-induced effects are assumed linear for the elastic constants,[16–21] the phonon frequencies, and for the crystal volume. In actual numerical calculation of the parameters at P_t (see Table I), a slightly modified nonlinear least-squares-fitting procedure of Vandevyer and Plumelle[52] was adopted. In this approach, we employ the calculated phonon energies as input and vary their values slightly while the known elastic and lattice constants are used as constraints. To understand the significance of the *two* sets of model parameters and to evaluate the dynamical properties of semiconductors at any desired pressure we used a linear interpolation equation

$$\alpha_i(P\neq 0)=\alpha_i(P=0)+P\frac{d\alpha_i}{dP}, \tag{10}$$

where α_i are the eleven RIM parameters.

B. Lattice dynamics, density of states, and Debye temperature

Using the parameter values of Table I along with the interpolation Eq. (10), we are now able to calculate the

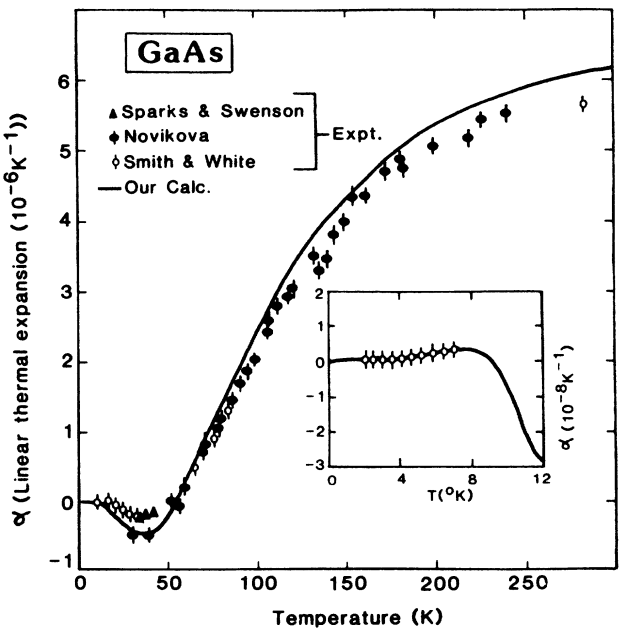

FIG. 7. Variation of linear thermal-expansion coefficient $\alpha(T)$ with temperature for GaAs. Experimental data are taken from Refs. 22 and 23.

pressure-dependent phonon properties of III-V compounds at any desired P. In Figs. 1 and 2, we have reported our calculations for the phonon dispersions $\omega_i(\mathbf{q})$ of GaP and GaAs along high symmetry ([ζ00], [$\zeta\zeta$0], and [$\zeta\zeta\zeta$]) directions (both at ambient pressure and P_t) and compared the results with the existing inelastic neutron scattering and/or the optical data.[37–42] Similar calculations for other compounds have also been performed. A satisfactory agreement of $\omega_i(\mathbf{q})$ both for $P=0$ (Refs. 37–42) and P_t (Refs. 10–15) is quite eminent. From Figs. 1 and 2, we have noticed some general trends in the calculated critical point phonons to be stated more precisely as follows. (i) The energies of the zone-boundary and near-zone-boundary TA phonons from the lowest branch decrease or soften with pressure P. The shifts of the TA(X) and TA(L) phonons are typical of the effect seen in other large $\mathbf{q}$ phonons from this branch. (ii) The energy of the LA(X) and LA(L) phonons increase with pressure. This increase is in agreement with our earlier results on II-VI tetrahedral compound semiconductors.[35] (iii) The optical phonons at the center (Γ point) of the Brillouin zone shift in higher energies with pressure. The transverse optical phonon [TO(Γ)] is found to shift faster than the longitudinal [LO(Γ)] for each material so that the splitting $[\omega_{\mathrm{LO}(\Gamma)}-\omega_{\mathrm{TO}(\Gamma)}]$ decreases with pressure. This (LO-TO) splitting, related directly to e_T^* via Eq. (5), is an intuitively expected result, since as the interatomic distance shortens with pressure it causes stiffening in the short range forces (see Table I) and results in less transfer of charge for the compressed crystal causing thereby a decrease in e_T^*. We have also verified the decrease of e_T^* in GaAs and GaP by Eq. (7) and using the pressure-dependent data for the dielectric constants.

Again, the knowledge of phonon frequencies $\omega_i(\mathbf{q})$ and phonon eigenvectors $e_\alpha(\kappa|\mathbf{q}i)$ enable us to calculate (using Green's function theory) a number of important vibrational properties of both perfect and imperfect semiconductors.[32] Comparisons of our theoretical results with the existing experimental[32] data for such physical quantities provided additional check on the coherence and on the reliability of our phenomenological scheme. The calculated one- (not shown here) and two- (see Figs. 3 and 4 for GaP and GaAs, respectively) phonon density of states for $P=0$ and $P\neq0$ designate several features observed in the first- and second-order Raman scattering spectra.[10–15] The pressure-dependent density of states maintains the general shape and exhibits accurately the shifts of the participating phonons in the additive and subtractive processes.[10–15] These shifts are consistent with the characteristic temperature dependence and polarization selection rules. The behavior of combination and difference modes involving TA phonons is particularly interesting due to the negative pressure coefficients of the latter. Combinations of these with optical phonons tend to have small pressure coefficients whereas difference modes with TO-TA have larger positive pressure coefficients (see Figs. 3 and 4).

Comparison of the calculated Debye temperature as a function of T at ambient pressure[56] (see Fig. 5 for GaAs) with the existing experimental results not only provides the reliability of our RIM11 but increases our confidence that we are able to predict similar results for $P\neq0$ (up to and including the transition pressure). From the calculated pressure-dependent results of the Debye temperature, it may be noted that the Θ values decrease in the low-T region and increase in the high-T region. Similar to the Grüneisen constant $\bar{\gamma}(T)$ and thermal-expansion coefficient $\alpha(T)$, the above results for $\Theta(T)$ give an excellent signature for the observed pressure-dependent phonon shifts [negative for the low-frequency (TA) and positive for the high-frequency (LA, LO, and TO) phonons] in III-V compound semiconductors.

C. Mode Grüneisen parameters and thermal expansion

The calculated values of $\omega_i(\mathbf{q})$ and $d\omega_i(\mathbf{q})/dP$ as a function of wave vector $\mathbf{q}$ throughout the Brillouin zone are used in Eq. (3) to study the variation of mode Grüneisen parameters $\gamma_i(\mathbf{q})$. The results along high-symmetry directions [ζ00], [$\zeta\zeta$0], and [$\zeta\zeta\zeta$] for GaAs are displayed in Fig. 6. The values of mode Grüneisen parameter at critical points for various III-V compounds are also reported in Table III and compared with the existing experimental[10–15] and theoretical[57] data. In almost all the cases, the agreement of our calculated results with the optical measurements reported by Cardona and his co-workers[10–15] is very encouraging. Except for the transverse acoustical phonons at X and L critical points where the mode Grüneisen parameters are negative, the values of γ's for other critical point phonons are found to be positive. It is believed that the lattice softening of the TA phonons is primarily responsible for the observed negative thermal-expansion coefficient $\alpha(T)$ (Refs. 22 and 23) in semiconductors.

Using the calculated values for $\gamma_i(\mathbf{q})$ in Eq. (3), we have evaluated the average Grüneisen constant $\bar{\gamma}(T)$ and then converted it to the temperature dependence of the linear thermal-expansion coefficient $\alpha(T)$. The contributions from the TA modes with small energies and large negative mode Grüneisen parameters (γ_{TA}) are found dominant in the calculated thermal-expansion coefficients at low temperatures. In Fig. 7, the theoretical results for $\alpha(T)$ for GaAs are compared with the existing experimental[22,23] data. For other compounds, we have also included in Table IV the results of α_{min} and $d\Theta/dP$ (at 300 K). Considering the simplicity of RIM11, the accurate prediction of the temperature region where the $\alpha(T)$ should attain negative and/or positive values has been very clearly reflected in our study.

IV. DISCUSSION AND CONCLUSIONS

A comprehensive study for the pressure-induced vibrational properties in III-V compound semiconductors is reported using a realistic lattice dynamical model in the *quasiharmonic approximation*. In this *macroscopic* approach, once the pressure dependence of model parameters in a solid is accurately established, nearly all of its vibrational properties at $P\neq0$ can be predicted with reasonable success. In III-V compounds, the calculated frequencies $\omega_i(\mathbf{q})$, one- and two-phonon densities of states, mode-Grüneisen-parameter dispersion curves, Debye temperature, and thermal-expansion coefficients are

all shown to be in good agreement with the existing experimental data.[10–23]

As a comparable case of GaAs, our results for mode Grüneisen parameters corroborate reasonably well with the existing experimental results and they fit relatively better than the existing cumbersome total-energy calculation[28] performed in the LDF formalism. It is to be mentioned, however, that unlike neutron scattering data at ambient pressure, our calculated phonon dispersions at P_t do not show the flatness (cf. Figs. 1 and 2) of the lowest TA branches. For the lattice dynamics of elemental semiconductors at $P=0$, Weber[58] has introduced a four-parameter dynamic bond-charge model (BCM) which successfully represented the zone-boundary TA phonons. In his study, the author of Ref. 58 has considered the following interactions in the BCM: (i) the nearest-neighbor central-force constant, (ii) a Coulomb interaction between the bond charge and the ion, (iii) a central interaction between ion and bond charge, and (iv) an interaction between bond charges. The flattening of the TA branches is obtained when the interaction (iv) is much larger than (ii) and (iii). Rustagi and Weber[59] have extended the BCM to III-V compounds by adding an additional parameter which measures the shift of the bond charge from the center towards the group-V ion. There is no reason why this model could not be employed to treat the high-pressure dispersion curves in elemental and compound semiconductors. This has not yet been attempted. However, we on the basis of our present calculations predict that for III-V compounds under pressure the bond charge should move adiabatically towards the center of the bond, leading to an increase in the covalency (or decrease in ionicity) of the bond. The use of BCM would also be appropriate, to resolve the issue whether the bending of the TA branches under compression is an *artifact* of our phenomenological RIM11 scheme or the peculiarity of the compound semiconductors.

In studying the variation of $\gamma(T)$ with temperature (γ_0 and γ_∞) for ionic solids, Born[45] used a repulsive potential between all unlike and an attractive potential between like ions. To predict the marked decrease in γ at low temperature, he also approximated the vibrational spectrum with acoustic and optic components of Debye and Einstein types, respectively. Following a better lattice-dynamical treatment of Barron[43] with repulsive potential of the form λr^{-n}, Blackman[60] argued that in solids the amount of variation in the Grüneisen constant γ_0 is much wider and extends to negative values with increasing n. This also suggests that in ionic solids $(\gamma_\infty-\gamma_0)$ is positive and larger. The negative value of γ_0 for the rock-salt structure had been obtained for transverse modes dependent on the elastic constant c_{44}. By increasing the repulsive exponent n, the ratio c_{44}/c_{11} could be diminished, thus weighing these modes more heavily at low temperatures. At the same time, the mode Grüneisen parameter became negative $\gamma_0=-0.62$ for $n=21$—a prediction which predated by several years the experimental discovery (see Ref. 8) in RbI. In sphalerite (ZnS) crystal since the negative value of the Grüneisen constant was already known, it was the shear modulus $C'=\frac{1}{2}(C_{11}-C_{12})$ that played an important role indicating that the negative γ_0 should be associated with open crystal structure and low shear moduli. Recent measurements and our realistic calculations in several elemental and compound semiconductors have made it possible to explicitly demonstrate Blackman's conjecture. In diamond–zinc-blende type crystals, the observed values of γ_0 range down from ~ 0.5 for Ge,[61] to ~ -2.0 for CuCl.[62] We may state a simple correlation between the value of γ_0 and the degree of ionicity (covalency) in the following way. For covalently bonded Ge, the shear moduli are stiffened by the angular forces, which can resist bond bending and consequently reduce their tendency to soften under pressure. With increasing ionicity, the nonuniformity of the charge distribution along the covalent bonds will cause weakening in the angular forces. Thus for highly ionic CuCl, the mode Grüneisen parameter for the lowest shear modes will become increasingly negative. Similar arguments of a balance between the weighted γ_i for the acoustic shear and the compressional modes can be applied in crystals to interpret the negative thermal expansion at low temperature; the former having a tendency towards negative values, whereas the latter are positive. In a lattice dynamical study, the description of $\alpha(T)$ [or $\bar{\gamma}(T)$] arises from the wave-vector dependence of the mode Grüneisen parameter $\gamma_i(\mathbf{q})$, related closely to the frequency spectrum of the crystal. At low temperatures, where the acoustic vibrations are dominant, the $\alpha(T)$ [or $\bar{\gamma}(T)$] becomes negative when the pressure or volume derivatives of TA phonons are negative (as seen in the present III-V compounds[22,23]). Despite the reasonable description of low-temperature results for $\alpha(T)$ (cf. Fig. 7) and $\bar{\gamma}(T)$ (not shown here), our theoretical calculations deviate from the existing experimental data at high temperatures. This may be attributed primarily due to the neglect of the anharmonic forces in our model calculations and partly due to the diversity in the existing experimental[10–15,63,64] pressure-dependent results for the optical phonons. Therefore, more experimental data and theoretical calculations (by including the effects of anharmonicity) are very much needed to understand the high-temperature results for the Grüneisen constant and linear thermal-expansion coefficient in III-V compound semiconductors.

Under compression, almost all solids exhibit *one* or *more* phase transformations causing drastic changes in their volume, symmetry, and electronic properties. It is well known that group-IV semiconductors transform under pressure from an insulating diamond to a metallic β-Sn structure, whereas most of the II-VI compound semiconductors transform into an insulating rock-salt phase. For III-V compounds, however, the situation is rather unclear. Neither theories[26–28] nor experiments[10–15] have been able to determine the structure of the high-pressure phase conclusively, although there are speculations that the behavior should be similar to the group-IV elements. Recent experiments[63] have indicated, however, that InSb crystallizes in the NaCl-structure and the pressure-induced x-ray measurements[64] suggested that GaAs may have transformed into a distorted NaCl crystal structure. These structures are, in all cases, believed to be metallic. Raman scattering spectroscopy is one of the nondestructive techniques that helps identifying the reduced symme-

try and yields antecedent behavior to the phase transition, by providing information of those lattice modes which soften under pressure. While calculating the pressure derivatives of various lattice modes we found positive values, consistent with the existing Raman data, for the optical [$\omega_{TO(\Gamma)}$ or $\omega_{LO(\Gamma)}$] phonons. This corresponds to (cf. Table I) an increase in the short-range interaction and to a decrease in the long-range Coulomb interaction. It is also clear (cf. Table III) that if this is the rule for zone-center phonons, the opposite rule is equally valid for the transverse acoustic zone boundary phonons for which the pressure coefficients of $\omega_{TA(X \text{ or } L)}$, are found negative. The question as to what extent this softening of the TA phonons is responsible for the high-pressure phase transition in semiconductors is not very clear at this time. Mitra and co-workers[65,66] and Weinstein[67] had tried to correlate these negative pressure coefficients to P_t, induced by pressure and driven by the transverse acoustical phonons. This was not confirmed by experiments[68–71] since in some cases the results were obtained at P very close to the transition pressure. For instance, Weinstein and Piermarini[13] performed experiments up to 120 kbar on Si (where P_t is ~ 125 kbar) and found TA(X) frequency exceeding 100 cm^{-1} at that pressure. In the same line of thought, Saunderson[71] performed pressure-dependent neutron measurements on RbI up to 3.8 kbar (within 200 bar of the phase transition) and found a negative Grüneisen parameter $\gamma_{TA(X)} = -3.35$, which resulted in a value for the TA mode exceeding 60% of its ambient pressure value. From this, it is quite clear that the above behavior near P_t is an intrinsic property of the shear distortion involved in the TA modes as mentioned before. The calculated results of the Grüneisen parameters $\gamma_{TA(X \text{ or } L)}$ (or related indirectly to the relative frequency shifts) for the III-V compound semiconductors are summarized in Table IV, together with the data on α_{min}, $d\Theta/dP$ (at 300 K), and P_t. The values reported in Table IV do not discriminate clearly which TA phonon softening (X or L) is predominant, although our results provide qualitative support (with the exception of GaAs, GaSb, and InP) to Weinstein's suggestion that the faster TA(X) frequency decreases with pressure for a compound, the lower its transition pressure. Again, the linear relation between $\gamma_{TA(X)}$ and P_t does not necessarily have the proper background from the electronic theory of solids and is not essential to the mechanism of the pressure-induced phase transition. We on the other hand believe that the LDF formalism should be able to elucidate possible connection, if any, between the zone boundary TA modes and the P_t. This point has not been fully explored despite the claim by Kunc and Martin[28] that the total energy of GaAs as a function of TA(X) eigenvector amplitude acquires a new minimum at elevated pressure. The uniqueness of this minimum has, however, not been completely examined. More work is therefore very much needed in this important area of research.

ACKNOWLEDGMENTS

The authors wish to express their sincere thanks to Dr. Bernard A. Weinstein, Dr. M. H. Manghnani, Dr. Karél Kunc, Dr. Michel Zigone, Dr. Gérard Martinez, and Professor M. Cardona for their interest and encouragements throughout the course of the present work. One of us (D.N.T.) is thankful to the authorities at Centre d'Etudes Nucléaires de Saclay, Gif-sur-Yvette, France for providing him with the opportunity to work in the Département de Physico-Chimie where a portion of the present work was completed and for the generous funds given to use of their computer facilities. The work is also partially supported by a U.S. National Science Foundation (NSF) grant to use Pittsburgh Supercomputer Facility and a grant from the Texas Advanced Technological Research Program through the University of Houston–University Park, Houston, Texas.

[1] M. Mizuta, M. Tachikawa, H. Kukimoto, and S. Minomura, Jpn. J. Appl. Phys. **24**, L143 (1985).

[2] R. A. Stradling, in Festkörperprobleme *(Advances in Solid State Physics)*, edited by P. Grosse (Pergamon/Vieweg, Braunschweig, 1985), Vol. XXV, p. 591.

[3] S. Porowski, *Proceedings of the 4th International Conference on the Physics of Narrow Gap Semiconductors, Linz, 1980,* edited by E. Gornick, H. Henrich, and L. Palmetshofer (Springer, Berlin, 1980), p. 420; L. Konczewicz, E. L. Staszewska, and S. Porowski, in *Proceedings of the 3rd International Conference on Narrow Gap Semiconductors, Warsaw, 1977,* p. 211.

[4] B. Welber, M. Cardona, Y. F. Tsay, and B. Bendow, Phys. Rev. B **15**, 875 (1977).

[5] T. Kobayashi, T. Tei, K. Aoki, K. Yamamoto, and K. Abe, in *Physics of Solids Under High Pressure,* edited by J. S. Schilling and R. N. Shelton (North-Holland, Amsterdam), 1981, p. 141.

[6] B. A. Weinstein and R. Zallen, in *Light Scattering in Solids,* Vol. IV of *Springer Series Topics in Applied Physics,* edited by M. Cardona and G. Güntherodt (Springer-Verlag, Berlin, 1984).

[7] A. Jayaraman, Rev. Mod. Phys. **55**, 65 (1983).

[8] T. H. K. Barron, J. G. Collins, and G. K. White, Adv. Phys. **29**, 609 (1980).

[9] K. R. Hirsch and W. B. Holzapfel, Rev. Sci. Instrum. **52**, 52 (1981).

[10] R. Trommer, E. Anastassakis, and M. Cardona, in *Light Scattering in Solids,* edited by M. Balkanski, R. C. C. Leite, and S. P. S. Porto (Flammarion, Paris, 1976), p. 396.

[11] R. Trommer, H. Müller, M. Cardona, and P. Vögl, Phys. Rev. B **21**, 4869 (1980).

[12] B. A. Weinstein, J. B. Renucci, and M. Cardona, Solid State Commun. **12**, 473 (1973).

[13] B. A. Weinstein and G. Piermarini, Phys. Rev. B **12**, 1172 (1975).

[14] D. Olego and M. Cardona, Phys. Rev. B **25**, 1151 (1982).

[15] D. Olego, M. Cardona, and P. Vögl, Phys. Rev. B **25**, 3878 (1982).

[16] D. N. Nichols, D. S. Rimai, and R. J. Sladek, Solid State Commun. **36**, 667 (1980).

[17] D. A. Swyt, Case Western Reserve University, Report No.

C00-623-167, 1971. Available from National Technical Information Service, Springfield, VA 22151.
[18]H. J. McSkimin, A. Jayaraman, P. Andreatch, Jr., and T. B. Bateman, J. Appl. Phys. **39**, 4127 (1968); H. J. McSkimin, A. Jayaraman, and P. Andreatch, Jr., *ibid.* **38**, 2362 (1967).
[19]G. I. Peresada, Fiz. Tverd. Tela (Leningrad) **14**, 1795 (1972) [Sov. Phys.—Solid State **14**, 1546 (1972-73)].
[20]Y. K. Yogurtcu, A. J. Miller, and G. A. Saunders, J. Phys. Chem. Solids **42**, 49 (1981).
[21]D. S. Rimai and R. J. Sladek, Solid State Commun. **30**, 591 (1979).
[22]S. I. Novikova, Fiz. Tverd. Tela (Leningrad) **2**, 2341 (1960) [Sov. Phys.—Solid State **2**, 2087 (1961)]; **3**, 178 (1961) [**3**, 129 (1961)]; **5**, 2138 (1963) [**5**, 1558 (1964)]; also in *Semiconductors and Semimetals* (Academic, New York, 1967), Vol. 3, p. 33.
[23]P. W. Sparks and C. A. Swenson, Phys. Rev. **163**, 779 (1967); T. F. Smith and G. K. White, J. Phys. C **8**, 2031 (1975).
[24]T. Soma, J. Satoh, and H. Matsuo, Solid State Commun. **42**, 889 (1982); T. Soma and K. Kudo, J. Phys. Soc. Jpn. **48**, 115 (1980).
[25]C. Patel, W. F. Sherman, and G. R. Wilkinson, J. Mol. Struct. **79**, 297 (1982).
[26]S. Froyen and M. L. Cohen, Solid State Commun. **43**, 447 (1982).
[27]M. T. Yin and M. L. Cohen, Phys. Rev. Lett. **45**, 1004 (1980).
[28]K. Kunc and R. Martin, Phys. Rev. B **24**, 2311 (1981).
[29]M. Scheffler, Physica B+C (Amsterdam) **146B**, 176 (1987).
[30]J. Dabrowski and M. Scheffler, Phys. Rev. Lett. **60**, 2183 (1988).
[31]D. J. Chadi and K. J. Chang, Phys. Rev. Lett. **60**, 2187 (1988).
[32]D. N. Talwar, M. Vandevyver, K. K. Bajaj, and W. M. Theis, Phys. Rev. B **33**, 8525 (1986).
[33]M. Zigone, M. Vandevyver, and D. N. Talwar, Phys. Rev. B **24**, 5763 (1981).
[34]W. M. Theis, D. N. Talwar, M. Vandevyver, and W. G. Spitzer, J. Appl. Phys. **58**, 2553 (1985).
[35]D. N. Talwar, M. Vandevyver, K. Kunc, and M. Zigone, Phys. Rev. B **24**, 741 (1981).
[36]K. Kunc, Ann. Phys. (Paris) **8**, 319 (1973–1974).
[37]G. Dolling, in *Symposium on Inelastic Scattering of Neutron in Solids and Liquids* (IAEA, Vienna, 1963), Vol. II, p. 37; G. Dolling and J. L. Waugh, *Lattice Dynamics,* edited by R. F Wallis (Pergamon, Oxford, 1965), p. 19.
[38]J. L. Yarnell, J. L. Warren, R. G. Wenzel and P. J. Dean, in *The Fourth IAEA Symposium on Inelastic Neutron Scattering* (IAEA, Vienna, 1968), Vol. I, p. 301.
[39]M. K. Faar, J. G. Traylor, and S. K. Sinha, Phys. Rev. B **11**, 1587 (1975).
[40]P. H. Borcherds, G. F. Alfrey, D. H. Saunderson, and A. D. B. Woods, J. Phys. C **8**, 2022 (1975).
[41](a) N. S. Orlova, Phys. Status Solidi B **103**, 115 (1981); (b) R. Charles, N. Saint-Cricq, J. B. Renucci, and A. Zwick, Phys. Rev. B **22**, 4804 (1980).
[42]D. L. Price, J. M. Rowe, and R. M. Nicklow, Phys. Rev. B **3**, 1268 (1971).
[43]T. H. K. Barron, Ann. Phys. (N.Y.) **1**, 77 (1957).
[44]E. Grüneisen, Ann. Phys. (Leipzig) [Folge 4] **39**, 257 (1912); Handb. Phys. **10**, 1 (1926).
[45]M. Born and K. Huang, *Dynamical Theory of Crystal Lattices* (Oxford University Press, New York, 1954), Chap. 2.
[46]G. Leibfreid and W. Ludwig, in *Solid State Physics* (Academic, New York, 1966), Vol. 12, 276.
[47]D. C. Wallace, Phys. Rev. **176**, 832 (1968); J. Appl. Phys. **41**, 5055 (1970).
[48]D. C. Wallace, *Thermodynamics of Crystals* (Wiley, New York, 1972).
[49]P. Plumelle, Ph.D. thesis, Université Pierre et Marie Curie, Paris, France, 1979.
[50]M. Vandevyver and P. Plumelle, Phys. Rev. B **17**, 675 (1978).
[51]D. N. Talwar, M. Vandevyver, and M. Zigone, J. Phys. C **13**, 3775 (1980).
[52]P. Plumelle and M. Vandevyver, Phys. Status Solidi B **73**, 271 (1976).
[53]M. Vandevyver and P. Plumelle, J. Phys. Chem. Solids **38**, 765 (1977).
[54]M. Zigone, Ph.D. thesis, Université Pierre et Marie Curie, Paris, France, 1981.
[55]F. D. Murnaghan, Proc. Nat. Acad. Sci. U.S.A. **30**, 244 (1944).
[56]U. Piesberger, Z. Naturforsch. **18a**, 141 (1963); in *Semiconductors and Semimetals,* edited by A. C. Beer and R. K. Willardson (Academic, New York, 1966), Vol. 2, p. 49.
[57]T. Soma and H. M. Kagaya, Phys. Status Solidi B **121**, K1 (1984).
[58]W. Weber, Phys. Rev. B **15**, 4789 (1977).
[59]K. C. Rustagai and W. Weber, Solid State Commun. **18**, 673 (1976).
[60]M. Blackman, Proc. Phys. Soc. London Sect. B **70**, 827 (1957); Philos. Mag. **3**, 831 (1958).
[61]C. J. Buchenauer, F. Cerdeira, and M. Cardona, in *Light Scattering in Solids,* edited by M. Balkanski (Flammarion, Paris, 1971), p. 280.
[62]G. A. Slack and P. Anderson, Phys. Rev. B **26**, 1873 (1982).
[63]O. Shimomura, K. Asaumi, N. Sakai, and S. Minomura, Philos. Mag. **34**, 839 (1976).
[64]A. L. Rouff and M. A. Baublitz, Jr., in *Physics of Solids Under Pressure,* edited by J. S. Schilling and R. N. Shelton (North-Holland, Amsterdam, 1981), p. 81.
[65]S. S. Mitra and K. V. Namjoshi, J. Chem. Phys. **55**, 1817 (1971); S. S. Mitra, C. Postmus, and J. R. Ferraro, Phys. Rev. Lett. **18**, 455 (1967); Phys. Rev. **186**, 942 (1969).
[66]J. F. Vetelino, S. S. Mitra, and K. V. Namjoshi, Phys. Rev. B **2**, 967 (1970).
[67]B. A. Weinstein, Solid State Commun. **20**, 999 (1976).
[68]W. A. Harrison, *Electronic Structure and the Properties of Solids* (Freeman, San Francisco, 1980).
[69]P. Vögl, J. Phys. C **11**, 251 (1976).
[70]G. A. Samara, Phys. Rev. B **27**, 3494 (1983).
[71]D. H. Saunderson, Phys. Rev. Lett. **17**, 530 (1966).

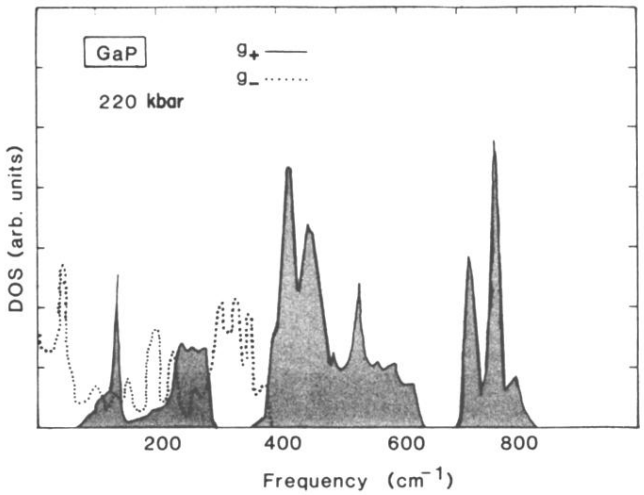

FIG. 3. Calculated two-phonon subtractive (· · ·) and additive (——) density of states for GaP. The major peaks show the shift of participating critical-point phonons under compression. The shift in optical phonons are consistent with the existing Raman data (see text).

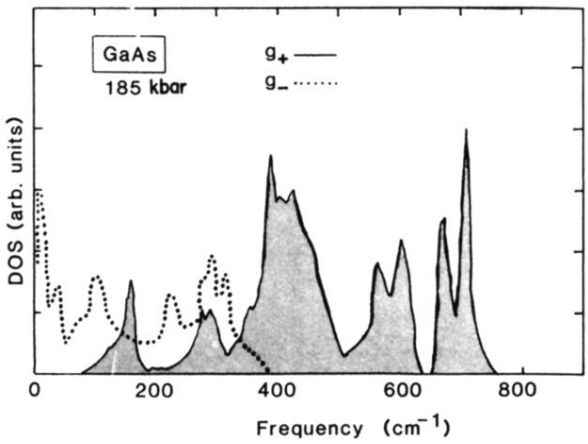

FIG. 4. Same key as of Fig. 3 for GaAs.